Advances in Nano Research, *Vol. 11, No. 2 (2021) 157-171*
https://doi.org/10.12989/anr.2021.11.2.157

Free vibration analysis of carbon nanotube RC nanobeams with variational approaches

Emrah Madenci*

Department of Civil Engineering, Necmettin Erbakan University, 42140 Konya, Turkey

(*Received February 6, 2021, Revised May 21, 2021, Accepted May 22, 2021*)

Abstract. There is not enough mixed finite element method (MFEM) model developed for dynamic analysis of carbon nanotube reinforced (CNTRC) composite beams in the literature. In the present study, free vibration analysis of functionally graded carbon nanotube reinforced composite (FG-CNTRC) nanobeams is carried out in the framework of variational formulations. The rule of mixture is employed to estimate the effective material properties of single-walled CNT reinforced nanobeams. Four kinds of CNT distribution of un-axially aligned reinforcement material are investigated in the through-thickness direction of the nanobeams. There are the uniform distribution (UD) and functionally graded distributions FG-O, FG-X and FG-Λ of CNTs in the thickness direction of the nanobeams (z axis direction) are assumed here for the analysis. The Hamilton's principle is used to derive governing differential equations based on trigonometric shear deformation beam theory. The effective functional has been constituted for FG-CNTRC nanobeams through a scientific procedure based on the Gâteaux differential. A simple mixed finite element formulation is utilized for the formulation of free vibration problems of FG-CNTRC nanobeams with different boundary conditions. The results of the present method are compared with others from the literature where a good agreement has been found. An effective energy functional and the mixed finite element formulation for FG-CNTRC nanobeams are the original contributions of this study.

Keywords: carbon nanotube; free vibration; functionally graded; high-order theory; mixed finite element method

1. Introduction

Recent advances in qualified new and advanced composite materials have placed more emphasis on the use of nanoscale reinforcing elements such as carbon nanotubes (CNTs) (Tounsi *et al*. 2013, Bouazza and Zenkour 2020). Due to the exceptional elastic, thermal, physical and electrical properties of CNTs, CNT-based composite materials have become the center of attention for application in various engineering composite structures (Kumar and Srinivas 2017). Excellent mechanical properties of carbon nanotubes, such as the extremely high elastic modulus, tensile strength, aspect ratio and low density, make them excellent candidate for the reinforcement of polymer composites. Nanomaterials are generally considered as the materials that have a characteristic dimension smaller than 100 nm (Hu *et al*. 2010, Hussain *et al*. 2019). The CNTs are single-walled and multi-walled which is synthesized by different techniques (Iijima and Ichihashi 1993, Wu *et al*. 2018a, b, Asghar *et al*. 2020a, b, Farazin and Mohammadimehr 2020, Ouakad *et al*. 2020). The single-walled CNT has a cylindrical shape that is continuously extruded with a single sheet of graphene about 1 nm in diameter and centimeter long (Bourada *et al*. 2020, Zerrouki *et al*. 2021). In contrast, multi-walled CNT has an array of such cylinders that are concentrically formed and separated by 0.35 nm, similar to basal plane separation in graphite with diameters of 2 nm to 100 nm and lengths of tens of microns (Liew *et al*. 2015, Asghar *et al*. 2020a, b). Many studies have been presented on the material properties of carbon nanotube reinforced composites (CNTRCs) (Khater and Abd el Gawaad 2016, Mehar *et al*. 2017, Bellal *et al*. 2020, Bendenia *et al*. 2020, Hussain *et al*. 2020, Rouabhia *et al*. 2020, Heidari *et al*. 2021). Structural complements such as plates, beams and membranes in micro or nano-length size are often employed as elements in micro/nano electro-mechanical systems (Boutaleb *et al*. 2019, Al-Furjan *et al*. 2020a, b, c, Huang *et al*. 2021).

In the past few decades, researchers have paid much attention to the development of CNTRC fiber reinforced composites. Conventional fibers are usually made from materials such as alumina, glass, boron and silicon carbide as fillers in fiber reinforced composites. These conventional fibers are in meso-scale with diameters of tens of microns and lengths of order of millimeters (Liew *et al*. 2015). The literature results on the CNTRC fiber reinforced composites demonstrated that in thicker matrix layers, reinforcement by adding a small proportion of nanotube leads to a significant improvement in beam stiffness and single-walled CNT buckles at smaller bending angles and greater flattening ratios (Vodenitcharova and Zhang 2006).

Today, nanotechnology is mainly concerned with the fabrication of nano-sized functionally graded materials (FGMs) and engineering structures, providing a new

*Corresponding author, Ph.D., Assistant Professor,
E-mail: emadenci@erbakan.edu.tr

ISSN: 2287-237X (Print), 2287-2388 (Online)

generation of breakthrough materials and enhanced functionality (Boukhari *et al*. 2016, Gemi *et al*. 2017, Al-Furjan *et al*. 2021a, b). The FGMs are a new breed of composite materials which are made of two or more constituent phases with properties that vary spatially according to a certain non-uniform distribution of the reinforcement phase (Liew *et al*. 2015, Al-Furjan *et al*. 2020a, b, c). The FGMs have some advantages over traditional composites due to the constant variability in material properties. For example, cracking and delamination phenomena can be avoided, stress concentrations and residual stresses can be minimized, and a smooth transition of distribution constraints can be achieved (Berghouti *et al*. 2019, Madenci 2019, Madenci and Gülcü 2020). The FGMs with engineered gradients of composition, structure or specific properties in the preferred direction/orientation are superior to traditional composite materials made of similar constituents because reinforcements are distributed either uniformly or randomly in the composites (Liew *et al*. 2015). Recently, Tounsi and his coworkers have investigated bending response, thermo-mechanical bending response, buckling and free vibration of FGMs (Ahmed Houari *et al*. 2011, Hadji *et al*. 2011, Merdaci *et al*. 2011, Taibi *et al*. 2015, Bouderba *et al*. 2016, Tounsi *et al*. 2016). With the rapid advancement of technology, FGMs are now widely used in micro/nonelectric mechanical systems. A number of micromechanics models such as the rule of mixture (Ebrahimi and Rostami 2018, Feng *et al*. 2020), Mori-Tanaka method (Moradi-Dastjerdi 2016, Rajabi and Mohammadimehr 2019), Halpin-Tsai method (Tahouneh 2017, Zhou *et al*. 2020), Hashin-Shtrikman bounds and Cox model, have been proposed for the determination of effective properties of FGMs. The mechanical properties of FG-CNTRCs have been extensively investigated experimentally, analytically and numerically (Akbaş 2016, 2018, Mohammadimehr and Alimirzaei 2017, Shafiei and Setoodeh 2017, Arani *et al*. 2018, 2019, Arefi *et al*. 2018, 2019, Kolahdouzan *et al*. 2018, Torabi and Ansari 2018, Wu *et al*. 2018a, b, Ebrahimi *et al*. 2019, Emdadi *et al*. 2019, Jamali *et al*. 2019, Al-Furjan *et al*. 2020a, b, c, 2021a, b, Civalek *et al*. 2020, Heidari *et al*. 2020). In the same context, based on the Euler-Bernoulli theory, first-order shear deformation (Timoshenko) and high-order shear deformation theories investigated in analytical studies. Zhu *et al*. (2012) studied the static and free vibrational analysis of the FG-CNTRC plates by using first-order shear deformation theory based on finite element method. The effective material properties of FG-CNTRC obtained according to the rule of mixture. Alibeigloo (2014) presented three types of FG distribution which are FG-X, FG-V and FG-O for the free vibration analysis of FG-CNTRCs by using the differential quadrature method. Wuite and Adali (2005) reported analyze of symmetric cross-ply and angle-ply laminated FG-CNTRC beams based on Euler-Bernoulli beam theory and developed according to the Mori-Tanaka method. Di Sciuva and Sorrenti (2019) investigated bending, free vibration and buckling analysis of FG-CNTRC plates using extended refined zigzag theory. The static and dynamic behavior of FG-CNTRC plates investigated and an effective formulation based on isogeometric analysis and higher-order shear deformation theory presented by Phung-Van *et al*. (2015). The subjected to uniaxial and biaxial in-plane mechanical loadings was investigated by using FSDT. They. Mehrabadi *et al*. (2012) concluded that CNTRC plates with symmetric distribution profile are the potential alternative to the plates with uniformly distributed (UD) CNTs and investigated buckling of FG-CNTRC rectangular plate based on first order shear deformation theory. Lin and Xiang (2014) proposed the vibration characteristics of CNTRC beams based on the first and high order shear deformation beam theories. Recently, the extensive usage of graphene structures subjected to different working conditions is also witnessed in the literature (Mahesh and Harursampath 2020, Vinyas and Harursampath 2020, Mahesh and Harursampath 2021). Magneto-electro-elastic materials and its composites are a class of smart or intelligent materials (Vinyas 2019a, b, 2020, Vinyas *et al*. 2019a, b, Vinyas and Dineshkumar 2020). Vinyas (2020a, b) studied the nonlinear coupled deflections of carbon nanotube (CNT) reinforced multiphase magneto-electro-elastic plates. A finite element procedure incorporating Reddy's higher order shear deformation theory and von Karman's nonlinear strain-displacement relation was employed to obtain governing equations. Vinyas *et al*. (2019a, b) investigated the problem of the three-dimensional free vibration behavior of skew magneto-electro elastic plates under the framework of a higher order shear deformation theory. To this end, the finite element method was adopted considering the Hamilton's principle. Recently, Arshid *et al*. (2021) conducted a throughout vibration analysis for sandwich microplates with a rectangular basis.

The Euler-Bernoulli beam theory disregards the effect of the transverse shear deformations and normal stresses. Because, the theory based on these assumptions; straight lines perpendicular to the transverse normal before deformation remain straight after deformation, the transverse normals are inextensible. So that it is only applied for thin beams, inapplicable for thick beams. Also, the first-order shear deformation theory does not neglect the transverse shear deformation effects that consider a uniform transverse shear stress distribution through the beam thickness with using a shear correction factor (Medani *et al*. 2019, Bousahla *et al*. 2020, Matouk *et al*. 2020). The shear correction factor dependents on layer orientation, loading conditions, geometric parameters and boundary conditions of beams. Therefore, it does not satisfy the condition of zero transverse shear stress at the surfaces of beam. The high-order shear deformation beam theories without the use of the shear correction factor have been developed to overcome all these deficiencies which are the function of the vertical coordinate components of the vertical displacement components (Balubaid *et al*. 2019). These theories does not neglect the effect of the transverse shear deformations and also satisfy the zero transverse shear stress on the surfaces of the beam because it includes nonlinear shear stress distributions provided by cubic (Ambartsumian 1958, Reissner 1975, Reddy 1984), trigonometric (Touratier 1991, Soldatos and Elishakoff 1992), hyperbolic (Grover *et al*. 2013, 2014), exponential

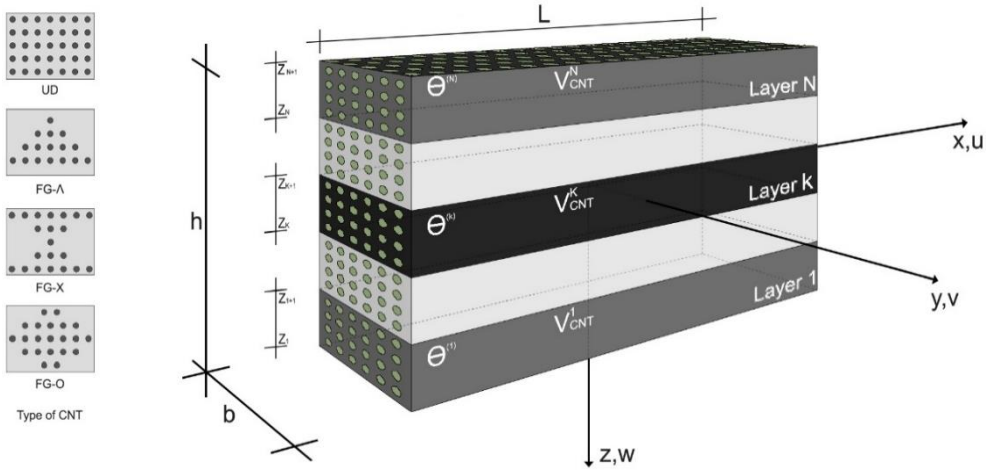

Fig. 1 FG-CNTRC beam model

(Karama *et al*. 2003, Aydogdu 2009) shear strain shape functions along the beam thickness.

Ritz method, Galerkin method, finite element method and differential squaring method are the most frequently used solution methods in the studies from past to present to obtain analysis results as stress, displacement, vibration or stability. The finite element method (FEM) which is a well-known and highly effective technique for the computation of approximate solutions of complex and boundary value problems. A FEM can only be considered in relation with a variational principle and a functional space (Kim *et al*. 2017, Vinyas 2019a, b, 2021, Vinyas *et al*. 2021). In the mixed type elements, besides the geometric quantities, depending on the assumptions used, the force and moment type magnitudes also contain variables (Özütok and Madenci 2013, Ozutok *et al*. 2014, Aribas *et al*. 2019, Madenci *et al*. 2020, Madenci and Özütok 2020).

It is observed from the literature review that there is no study available on static and free vibration analysis of FG-CNTRC nanobeams in the framework of the trigonometric shear deformation theory and mixed FEM solution in the existing literature till yet. In the present study, a mixed FEM model is developed to carry out free vibration analyses of FG-CNTRC nanobeams based on the trigonometric shear deformation theory. The beam is made of perfectly bonded CNTRC layers and in each layer single-walled CNT are assumed to be uniformly and FG distributions along the thickness directions. The effective material properties of CNTRCs are estimated through the rule of mixture in which the CNT efficiency parameters are introduced to account for the scale-dependence of the resulting nanostructures. In the kinematic equations of the element, a function that defines the trigonometric dispersion of shear deformations was used. In order to obtain equations of motion, energy methods were used with the Hamilton' principle. The influences of CNT volume fraction, width-to-thickness ratio and boundary conditions on natural frequencies are discussed for the FG-CNTRC nanobeams. After the field equations were shown to be compatible within themselves, a contemporary functional of composite beams based on trigonometric shear deformation theory involving dynamic and geometric boundary conditions was derived as in the study by Madenci (2019).

2. Theoretical formulations

2.1 Effective material properties of FG-CNTRC nanobeams

In this paper, four types of FG-CNTRC beams with length "*L*", width "*b*" and thickness "*h*" were considered as shown in Fig. 1. It is assumed that a FG-CNTRC beam is made from a mixture of an isotropic matrix reinforced with single-walled (10,10) armchair CNTs either uniformly (UD), non-uniform FG-O, FG-X and FG-Λ distributions in beam thickness direction. CNT in FG-CNTRC layer are considered as aligned along the axial direction (0º), whereas fibers in composite are aligned in the transverse direction (90º). The effective material properties of FG-CNTRC can be defined according to the extended rule of mixtures for each distribution pattern as:

$$E_{11} = \eta_1 V_{CNT} E_{11}^{CNT} + V_m E_m \tag{1}$$

$$\frac{\eta_2}{E_{22}} = \frac{V_{CNT}}{E_{22}^{CNT}} + \frac{V_m}{E_{22}^{m}} \tag{2}$$

$$\frac{\eta_3}{G_{12}} = \frac{V_{CNT}}{G_{12}^{CNT}} + \frac{V_m}{G_m} \tag{3}$$

$$\nu_{12} = V_{CNT} \nu_{12}^{CNT} + V_m \nu_m \tag{4}$$

$$\rho = V_{CNT} \rho_{CNT} + V_m \rho_m \tag{5}$$

where "E_{11}^{CNT}, E_{22}^{CNT} and G_{12}^{CNT}" are Young's and shear modulus of the single-walled of the CNT, respectively. And "E_m and G_m" represent the corresponding properties of the isotropic matrix. To account for the scale-dependent material properties, "η_i $(i = 1,2,3)$" are CNT/matrix efficiency parameters which can be determined by matching the effective properties of CNTRC observed from the molecular dynamics simulations with the predictions of the extended rule of mixture. "ρ_{CNT} and ρ_m" are mass densities of the CNT and matrix, respectively. "V_{CNT} and

V_m" are the volume fractions of the CNT and matrix, respectively, and related by

$$V_{CNT} + V_m = 1 \tag{6}$$

The uniform (UD) and three different FG-O, FG-X and FG-Λ distributions of CNT along the thickness direction of the nanocomposite beams shown in Fig. 1 and are assumed to be as following:

$$V_{CNT}(z) = V_{CNT}^{*} \qquad \text{(UD)} \tag{7}$$

$$V_{CNT}(z) = \frac{4|z|}{h} V_{CNT}^{*} \qquad \text{(FG-X)} \tag{8}$$

$$V_{CNT}(z) = 2(1 - \frac{2|z|}{h}) V_{CNT}^{*} \qquad \text{(FG-O)} \tag{9}$$

$$V_{CNT}(z) = (1 - \frac{2z}{h}) V_{CNT}^{*} \qquad \text{(FG-}\Lambda\text{)} \tag{9}$$

where "V_{CNT}^{*}" is the total CNT volume fraction determined by

$$V_{CNT}^{*} = \frac{w_{CNT}}{w_{CNT} + \frac{\rho_{CNT}}{\rho_m} - \frac{\rho_{CNT}}{\rho_m} w_{CNT}} \tag{11}$$

where "w_{CNT}" is the mass fraction of the CNT in the composite nanobeams.

2.2 Displacement filed and strains of FG-CNTRC nanobeams

The trigonometric shear deformation beam theory was employed to account for the displacement. According to theory, the displacements of any point in the beam along the x-axis and z-axis, denoted by U(x,z,t) and W(x,z,t) respectively as follows (Touratier 1991)

$$\begin{aligned} u(x,z,t) &= u_0 - z\frac{\partial w_0(x,t)}{\partial x} + \psi(z)\gamma_0(x,t) \\ v(x,z,t) &= 0 \\ w(x,z,t) &= w_0(x,t) \end{aligned} \tag{12}$$

where "u_0" and "w_0" are the axial and transverse displacement at the reference plane of the beam, respectively. The "γ_0" is denote transverse shear strain at any point on the reference plane which can be defined as

$$\gamma_0(x,t) = \frac{\partial w_0(x,t)}{\partial x} - \phi_0(x,t) \tag{13}$$

where "ϕ_0" is the total bending rotation of the cross-section at any point of the reference plane. In Eq. (12), the "$\psi(z)$" is shape function which is indicating the transverse shear deformation and stress distribution through the thickness of the FG-CNTRC nanobeams. By considering "$\psi(z)$" for trigonometric shear deformation theory:

$$\psi(z) = \frac{h}{\pi}\sin\left(\frac{\pi}{z} - h\right) \tag{14}$$

Utilizing the displacement field expressed in Eq. (12), the normal and shear strain components associated with the displacement field are as follows
where

$$\begin{aligned} \varepsilon_{xx} &= \varepsilon_{xx}^{0} + z\varepsilon_{xx}^{1} + \psi(z)\varepsilon_{xx}^{2} \\ \gamma_{xz} &= g(z)\varepsilon_{xz}^{0} \end{aligned} \tag{15}$$

$$\begin{aligned} &\varepsilon_{xx}^{0} = \frac{\partial u_0}{\partial x}; \quad \varepsilon_{xx}^{1} = -\frac{\partial^2 w_0}{\partial x^2}; \quad \varepsilon_{xx}^{2} = (\frac{\partial \phi_0}{\partial x} + \frac{\partial^2 w_0}{\partial x^2}); \\ &\varepsilon_{xz}^{0} = (\phi_0 + \frac{\partial w_0}{\partial x}); \quad g(z) = \frac{\partial \psi(z)}{\partial z} = \cos(\frac{\pi z}{h}) \end{aligned} \tag{16}$$

2.3 Equations of motion of FG-CNTRC nanobeams

A variational approach on the basis of the Hamilton's principle is utilized to derive the governing equations as well as corresponding boundary conditions of FG-CNTRC nanobeams. To obtain the equations of motion, the Hamilton's principle is employed as following:

$$\int_{t_1}^{t_2} (\delta U + \delta V - \delta K) dt = 0 \tag{17}$$

where "δU", "δV" and "δK" are the virtual variation of total strain energy, work done by external loads and kinetic energy, respectively. The virtual strain energy of trigonometric shear deformable FG-CNTRC nanobeams can be expressed as

$$\begin{aligned} \delta U &= \int_0^L \int_A (\sigma_{xx}\delta\varepsilon_{xx} + \tau_{xz}\delta\gamma_{xz}) dA dx \\ &= \int_0^L (N_{xx}\delta\varepsilon_{xx}^{0} + M_{xx}\delta\varepsilon_{xx}^{1} + P_{xx}\delta\varepsilon_{xx}^{2} + Q_x\delta\varepsilon_{xz}^{0}) dx \end{aligned} \tag{18}$$

where the stress resultants terms "N_x", "M_x", "P_x" and "Q_{xz}" are the in-plane load, bending moment, higher-order generalized bending moment and shear force, respectively. All stress resultants are expressed as

$$N_x = \int_A \sigma_{xx} dA \tag{19a}$$

$$M_x = \int_A \sigma_{xx} z dA \tag{19b}$$

$$P_x = \int_A \sigma_{xx} \psi(x) dA \tag{19c}$$

$$Q_{xz} = \int_A \sigma_{xx} g(z) dA \tag{19d}$$

The kinetic energy is calculated for the dynamic case as follows

$$\delta K=\frac{1}{2}\int_0^L\begin{Bmatrix} I_0\left[\left(\frac{\partial u_0}{\partial t}\right)^2+\left(\frac{\partial w_0}{\partial t}\right)^2\right]+2I_1\frac{\partial u_0}{\partial t}\frac{\partial^2 w_0}{\partial t\partial x} \\ +2I_2\frac{\partial u_0}{\partial t}\frac{\partial \gamma_0}{\partial t}+2I_3\frac{\partial \gamma_0}{\partial t}\frac{\partial^2 w_0}{\partial t\partial x} \\ +I_4\left(\frac{\partial^2 w_0}{\partial t\partial x}\right)^2+I_5\left(\frac{\partial \gamma_0}{\partial t}\right)^2 \end{Bmatrix}dx \quad (20)$$

where the mass moments of the inertia defined as

$$\left[I_0,I_1,I_2,I_3,I_4,I_5\right]=\int_A \rho(z)\left\{1,z,z^2,\psi(z),z\psi(z),\psi^2(z)\right\}dA \quad (21)$$

The variation of work done by the external load can be obtained as

$$\delta V=-\int_0^L F(t,x)\delta w_0 dx \quad (22)$$

By substituting Eqs. (18), (20) and (22) into Eq. (17) and consequently utilizing the fundamental lemma of the calculus of variations, equations of motion for trigonometric shear deformable FG-CNTRC nanobeams are achieved in terms of the resultants are follows

$$\delta u_0:\frac{\partial N_{xx}}{\partial x}=I_0\frac{\partial^2 u_0}{\partial t^2}-I_1\frac{\partial^3 w_0}{\partial x\partial t^2}+I_3\left(\frac{\partial^3 w_0}{\partial x\partial t^2}-\frac{\partial^2 \phi_0}{\partial t^2}\right) \quad (23a)$$

$$\delta \phi_0:\frac{\partial P_{xx}}{\partial x}-Q_{xz}=I_3\frac{\partial^2 u_0}{\partial t^2}-I_4\frac{\partial^3 w_0}{\partial x\partial t^2}+I_5\left(\frac{\partial^3 w_0}{\partial x\partial t^2}-\frac{\partial^2 \phi_0}{\partial t^2}\right) \quad (23b)$$

$$\begin{aligned}\delta w_0:&\frac{\partial^2 P_{xx}}{\partial x^2}-\frac{\partial^2 M_{xx}}{\partial x^2}-\frac{\partial Q_{xz}}{\partial z}-q=-I_0\frac{\partial^2 w_0}{\partial t^2}-I_1\frac{\partial^3 u_0}{\partial x\partial t^2}\\&+I_2\frac{\partial^4 w_0}{\partial x^2\partial t^2}+I_3\frac{\partial^3 u_0}{\partial x\partial t^2}+I_4\left(\frac{\partial^3 \phi_0}{\partial x\partial t^2}-2\frac{\partial^4 w_0}{\partial x^2\partial t^2}\right)\\&+I_5\left(\frac{\partial^4 w_0}{\partial x^2\partial t^2}-\frac{\partial^3 \phi_0}{\partial x\partial t^2}\right)\end{aligned} \quad (23c)$$

2.4 Governing equations of FG-CNTRC nanobeams

The material constitutive equations are written under linear elastic deformations as

$$\sigma_{xx}=Q_{11}(z)\varepsilon_{xx}=\frac{E_{11}(z)}{1-\nu^2(z)}\varepsilon_{xx} \quad (24a)$$

$$\tau_{xz}=Q_{55}(z)\gamma_{xz}=G_{12}(z)\gamma_{xz} \quad (24b)$$

By substituting Eqs. (24a-b) into Eqs. (19a-d), the constitutive equations can be expressed in the form of material stiffness components and displacements as following

$$N_{xx}=A_{11}\frac{\partial u_0}{\partial x}-B_{11}\frac{\partial^2 w_0}{\partial x^2}+C_{11}\frac{\partial \gamma_0}{\partial x} \quad (25a)$$

$$M_{xx}=B_{11}\frac{\partial u_0}{\partial x}-D_{11}\frac{\partial^2 w_0}{\partial x^2}+E_{11}\frac{\partial \gamma_0}{\partial x} \quad (25b)$$

$$P_{xx}=C_{11}\frac{\partial u_0}{\partial x}-E_{11}\frac{\partial^2 w_0}{\partial x^2}+H_{11}\frac{\partial \gamma_0}{\partial x} \quad (25c)$$

$$Q_{xz}=A_{55}\gamma_0 \quad (25d)$$

where the rigidities "D_{11}" denote the bending stiffness, "B_{11}" denote the bending-extensional coupling stiffnesses, "C_{11}", "E_{11}" and "H_{11}" denote the high order stiffnesses, "A_{11}" and "A_{55}" denote the normal and high order extensional stiffnesses respectively, defined as follows

$$[A_{11},B_{11},D_{11}]=\int_A Q_{11}\,[1,z,z^2]dA \quad (26a)$$

$$[C_{11},E_{11}]=\int_A Q_{11}\psi(z)\,[1,z]dA \quad (26b)$$

$$[H_{11}]=\int_A Q_{11}\psi^2(z)\,dA \quad (26c)$$

$$[A_{55}]=\int_A Q_{55}g^2(z)\,dA \quad (26d)$$

Substituting the stress resultants of Eqs. (25) into Eqs. (23) yields the following reduced equations of motion or governing equations of FG-CNTRC nanobeams are generated

$$\begin{aligned}&A_{11}\frac{\partial^2 u_0}{\partial x^2}-B_{11}\frac{\partial^3 w_0}{\partial x^3}+C_{11}\frac{\partial^2 \gamma_0}{\partial x^2}\\&=I_0\frac{\partial^2 u_0}{\partial t^2}-I_1\frac{\partial^3 w_0}{\partial x\partial t^2}+I_3\frac{\partial^2 \gamma_0}{\partial t^2}\end{aligned} \quad (27a)$$

$$\begin{aligned}&C_{11}\frac{\partial^2 u_0}{\partial x^2}-E_{11}\frac{\partial^3 w_0}{\partial x^3}+H_{11}\frac{\partial^2 \gamma_0}{\partial x^2}-A_{55}\gamma_0\\&=I_3\frac{\partial^2 u_0}{\partial t^2}-I_4\frac{\partial^3 w_0}{\partial x\partial t^2}+I_5\frac{\partial^2 \gamma_0}{\partial t^2}\end{aligned} \quad (27b)$$

$$\begin{aligned}&C_{11}\frac{\partial^3 u_0}{\partial x^3}-E_{11}\frac{\partial^4 w_0}{\partial x^4}+H_{11}\frac{\partial^3 \gamma_0}{\partial x^3}-B_{11}\frac{\partial^3 u_0}{\partial x^3}\\&+D_{11}\frac{\partial^4 w_0}{\partial x^4}-E_{11}\frac{\partial^3 \gamma_0}{\partial x^3}-A_{55}\frac{\partial \gamma_0}{\partial x}-q\\&=-I_0\frac{\partial^2 w_0}{\partial t^2}-I_1\frac{\partial^3 u_0}{\partial x\partial t^2}+I_2\frac{\partial^3 w_0}{\partial x\partial t^2}+I_3\frac{\partial^3 u_0}{\partial x\partial t^2}\\&-I_4\left[\frac{\partial^3 \gamma_0}{\partial x\partial t^2}+\frac{\partial^4 w_0}{\partial x^2\partial t^2}\right]+I_5\frac{\partial^3 \gamma_0}{\partial x\partial t^2}\end{aligned} \quad (27c)$$

In this study only under distribution loads problems investigated so that extensional coupling stiffnesses are zero as "$A_{11}=B_{11}=C_{11}=0$".

2.5 Approximate with variational and mixed finite element formulation

The partial differential field equations can be transformed to functional with boundary conditions. The functional is obtained via Gateaux differential method. The field equations including boundary conditions for FG-CNTRC nanobeams can be written in operator matrices form as

$$\begin{bmatrix} [D] & [0]_{4\times5} \\ [0]_{5\times4} & \begin{matrix} 0 & 0 & 0 & 1 \\ 0 & 0 & 1 & 0 \\ 0 & -1 & 0 & 0 \\ -1 & 0 & 0 & 0 \end{matrix} \end{bmatrix} \begin{Bmatrix} [F] \\ [B] \end{Bmatrix} = \begin{bmatrix} q \\ 0 \\ 0 \\ 0 \\ 0 \\ [\hat{B}] \end{bmatrix} \tag{28}$$

where "$[D]$" is differential operator matrices, "$[F]$" is unknown freedoms matrices and "$[B]$ and $[\hat{B}]$" are dynamic and geometric boundary conditions matrices. The first matrices is the differential operator, the second matrices is the unknown freedoms and third matrices is the external influence vectors, respectively. These matrices can be written as

$$[D] = \begin{bmatrix} 0 & 0 & D_{11}\frac{\partial^2}{\partial x^2} & -E_{11}\frac{\partial^2}{\partial x^2} & 0 \\ 0 & 0 & E_{11}\frac{\partial}{\partial x} & -H_{11}\frac{\partial}{\partial x} & A_{55} \\ D_{11}\frac{\partial^2}{\partial x^2} & E_{11}\frac{\partial}{\partial x} & D_{11} & -E_{11} & 0 \\ -E_{11}\frac{\partial^2}{\partial x^2} & H_{11}\frac{\partial}{\partial x} & E_{11} & -H_{11} & 0 \\ 0 & -A_{55} & 0 & 0 & A_{55} \end{bmatrix}_{5\times5} \tag{29a}$$

$$[F] = \begin{bmatrix} w_0 \\ \gamma_0 \\ \left[\frac{E_{11}P_x - H_{11}M_x}{D_{11}H_{11} - E_{11}^2}\right] \\ \left[\frac{D_{11}P_x - E_{11}M_x}{D_{11}H_{11} - E_{11}^2}\right] \\ \left[\frac{Q_{xz}}{A_{55}}\right] \end{bmatrix}_{1\times5} \tag{29b}$$

The Gateaux derivative of an operator is defined as

$$dQ(\mathrm{y},\bar{\mathrm{y}}) = \left.\frac{\partial Q(y+\tau\bar{y})}{\partial\tau}\right|_{\tau=0} \tag{30}$$

A required and sufficient condition for **Q** to be a potential is;

$$< \mathrm{dQ}(\mathrm{y},\bar{\mathrm{y}}), y^* > \; = \; < \mathrm{dQ}(\mathrm{y},\mathrm{y}^*), \bar{y} > \tag{31}$$

If the operator **Q** is a potential, then the functional (Oden and Reddy 1976) corresponding to the field equations can be obtained as (Özütok and Madenci 2017)

$$\begin{aligned} I_{[y]} &= \left[\frac{\partial M_x}{\partial x}, \frac{\partial w_0}{\partial x}\right] + \left[P_x, \left(\frac{\partial \phi_x}{\partial x} + \frac{\partial^2 w_0}{\partial x^2}\right)\right] + \left[Q_{xz}, \left(\phi_x + \frac{\partial w_0}{\partial x}\right)\right] \\ &- \frac{F_{11}}{D_{11}H_{11} - E_{11}^2}\left[M_x, P_x\right] - \frac{1}{2A_{55}}\left[Q_{xz}, Q_{xz}\right] - \frac{H_{11}}{2[D_{11}H_{11} - E_{11}^2]}\left[M_x, M_x\right] \\ &- \frac{D_{11}}{[D_{11}H_{11} - E_{11}^2]}\left[P_x, P_x\right] - \left[q, w\right] + \left[(\hat{\mathrm{w}} - \mathrm{w}), \mathrm{R}\right]_{\varepsilon} + \left[(\hat{\Omega} - \Omega), \mathrm{M}\right]_{\varepsilon} \\ &- \left[\mathrm{R}, \mathrm{w}\right]_{\sigma} - \left[\hat{\mathrm{M}}, \Omega\right]_{\sigma} \end{aligned} \tag{32}$$

The mixed-type FE model is far more efficient due to variables can be chosen independently, the forces and moments can be calculated with less number of elements but more sensitive. The mixed-type FE method extensively used by researchers (Aköz and Kadioğlu 1996, 1999, Carrera 1998, Desai *et al*. 2003, Lage *et al*. 2004) for static and dynamic analyses of various composite beam, plate and shell elements. A close examination of the functional shows that usage of linear shape functions are allowed. The nodal degrees of freedom will be consisted convention for nodal displacement, rotations, moments and forces.

$$\begin{aligned} &\{\boldsymbol{U}\}_i^e \\ &= \left\{w_0; \quad \frac{\partial w_0}{\partial x}; \quad \gamma_0; \quad \frac{\partial \gamma_0}{\partial x}; \quad M_x; \quad \frac{\partial M_x}{\partial x}; \quad P_x; \quad Q_{xz}\right\} \end{aligned} \tag{33}$$

The variables can be written in vector form for one nanobeams element for with the two node element as

$$\{U\}_i^e = \{\{U\}_1^e; \{U\}_2^e\} \tag{34}$$

The linear interpolation functions in terms of "ζ" non-dimensional coordinates ($-1 \le \zeta \le +1$) are given as

$$\chi_{i;j} = \frac{1}{2}\,(1 \pm \zeta) \qquad i;j = 1;2 \tag{35}$$

The following submatrices are defined to give an explicit form of the element matrix for nanobeams

$$\left[k_{i,j}\right]_1 = \int_{-1}^{1}\{\chi_i \; \chi_j\}dx \qquad (i,j = 1,2) \tag{36a}$$

$$\left[k_{i,j}\right]_2 = \int_{-1}^{1}\left\{\frac{\partial \chi_i}{\partial x}\frac{\partial \chi_j}{\partial x}\right\}dx \qquad (i,j = 1,2) \tag{36b}$$

$$\left[k_{i,j}\right]_3 = \int_{-1}^{1}\left\{\chi_i \; \frac{\partial \chi_j}{\partial x}\right\}dx \qquad (i,j = 1,2) \tag{36c}$$

The mixed FEM matrices of FG-CNTRC nanobeams element based on trigonometric shear deformation theory which has total ten degree-of-freedom at the nodes is obtained as

$$[K] = \begin{bmatrix} 0 & 0 & 0 & 0 & \frac{1}{L} & -\frac{1}{L} & 0 & 0 & 0 & 0 \\ 0 & 0 & 0 & 0 & -\frac{1}{L} & \frac{1}{L} & 0 & 0 & 0 & 0 \\ 0 & 0 & 0 & 0 & 0 & 0 & -\frac{1}{2} & \frac{1}{2} & \frac{L}{3} & \frac{L}{6} \\ 0 & 0 & 0 & 0 & 0 & 0 & -\frac{1}{2} & \frac{1}{2} & \frac{L}{6} & \frac{L}{3} \\ \frac{1}{L} & -\frac{1}{L} & 0 & 0 & -\frac{H_{11}}{D_{11}H_{11}-E_{11}^2}\frac{L}{6} & -\frac{H_{11}}{D_{11}H_{11}-E_{11}^2}\frac{L}{12} & \frac{E_{11}}{D_{11}H_{11}-E_{11}^2}\frac{L}{3} & \frac{E_{11}}{D_{11}H_{11}-E_{11}^2}\frac{L}{6} & 0 & 0 \\ -\frac{1}{L} & \frac{1}{L} & 0 & 0 & -\frac{H_{11}}{D_{11}H_{11}-E_{11}^2}\frac{L}{12} & -\frac{H_{11}}{D_{11}H_{11}-E_{11}^2}\frac{L}{6} & \frac{E_{11}}{D_{11}H_{11}-E_{11}^2}\frac{L}{6} & \frac{E_{11}}{D_{11}H_{11}-E_{11}^2}\frac{L}{3} & 0 & 0 \\ 0 & 0 & -\frac{1}{2} & -\frac{1}{2} & \frac{E_{11}}{D_{11}H_{11}-E_{11}^2}\frac{L}{3} & \frac{E_{11}}{D_{11}H_{11}-E_{11}^2}\frac{L}{6} & -\frac{D_{11}}{D_{11}H_{11}-E_{11}^2}\frac{L}{6} & -\frac{D_{11}}{D_{11}H_{11}-E_{11}^2}\frac{L}{12} & 0 & 0 \\ 0 & 0 & \frac{1}{2} & \frac{1}{2} & \frac{E_{11}}{D_{11}H_{11}-E_{11}^2}\frac{L}{6} & \frac{E_{11}}{D_{11}H_{11}-E_{11}^2}\frac{L}{3} & -\frac{D_{11}}{D_{11}H_{11}-E_{11}^2}\frac{L}{12} & -\frac{D_{11}}{D_{11}H_{11}-E_{11}^2}\frac{L}{6} & 0 & 0 \\ 0 & 0 & \frac{L}{3} & \frac{L}{6} & 0 & 0 & 0 & 0 & -\frac{1}{A_{55}}\frac{L}{6} & -\frac{1}{A_{55}}\frac{L}{12} \\ 0 & 0 & \frac{L}{6} & \frac{L}{3} & 0 & 0 & 0 & 0 & -\frac{1}{A_{55}}\frac{L}{12} & -\frac{1}{A_{55}}\frac{L}{6} \end{bmatrix} \quad (37)$$

2.6 Free vibration analysis

For the free vibration analysis, the equation for the small harmonic oscillations of the FG-CNTRC nanobeams as

$$([K] - \lambda_i^2[M])\{U_i\} = \{0\} \quad i = 1,2,\dots,n \quad (38)$$

where "$[K]$" is the stiffness matrix, "$[M]$" is the mass matrix, the eigenvalue "$\lambda_i{}^2$" is the non-dimensional frequency and "$\{U\}$" is indicate the transverse vector. The non-trivial solution of Eq. (38) is only possible if the coefficients can be zero as

$$|[K] - \lambda_i^2[M]| = 0 \quad (39)$$

3. Numerical solutions

In this section results of mixed FEM formulation are verified in terms of free vibration of FG-CNTRC nanobeams via comparison with previous studies. In this study, poly methyl methacrylate, referred to PMMA, is used as the matrix and the armchair (10,10) single-walled CNTs are selected as reinforcements at room temperature (300 K). The material properties are given as Young's modulus $E = 2.5$ GPa, Poisson's coefficient $\nu = 0.3$, mass density $\rho = 1190$ kg/m^3 for matrix; Young's modulus$E_{11} = 600$ GPa, $E_{22} = 10$ GPa, Poisson's coefficient $\nu_{12} = 0.19$, mass density $\rho = 1400$ kg/m^3, shear modulus $G_{12} = 17.2$ GPa for CNT. The CNT efficiency parameters "η_i" associated with the given volume fraction "V_{CNT}^*" are shown in Table 1. It should be mentioned that the UD and other FG-CNT distributions nanobeams have the same mass fraction of CNT.

Four types of FG-CNTRC nanobeams UD; FG-Λ; FG-X and FG-O are considered with different boundary conditions which are simply-supported (SS), clamped-clamp (CC) and cantilever (CF). The non-dimensional parameter is defined as

$$\bar{\omega} = \omega \frac{L^2}{h}\sqrt{\frac{\rho_m}{E_m}} \quad (40)$$

Firstly, the effect of CNT distribution on the beam was examined on the material properties. The variation of longitudinal Young's modulus E_{11} along the beam thickness depends on the V_{CNT} * values. It was given on the 2nd. Accordingly, a symmetrical distribution occurred in the FG-O and FG-X models, while an unsymmetrical distribution occurred in the FG-Λ model. In the FG-O model, E11 in the top layer is 2.5 GPa while it is 186.6 GPa in the middle layer; 275.30 GPa and 445.90 GPa; FG-X model 370.90 GPa in the top layer; It is 548.1 GPa and 889.3 GPa while it is 2.5 GPa in the middle layer; The FG-Λ model is 2.5 GPa in the top layer and 186.6 GPa in the bottom layer; Maximum and minimum values of 275.30 GPa and 445.90 GPa were obtained.

For the second comparison study investigates the natural frequencies of FG-CNTRC nanobeams for different boundary conditions with width-to-thickness ratio L/h = 15. The non-dimensional first five frequency parameters of various types of FG-CNTRC nanobeams without layer and V_{CNT}* = 0.12 are listed in Table 2. Present mixed FEM results compared with FEM solutions and Ritz approximate solutions by Kumar and Srinivas (2017). Tables 3 and 4 show the non-dimensional natural frequency parameters for FG-CNTRC nanobeams, which are estimated for V_{CNT}* = 0.17 and V_{CNT}* = 0.28 volume fraction of CNT. Results

Table 1 The CNT efficiency parameters

V_{CNT}^*	η_1	η_2	η_3
0.12	1.2833	1.0556	1.0556
0.17	1.3414	1.7101	1.7101
0.28	1.3238	1.7380	1.7380

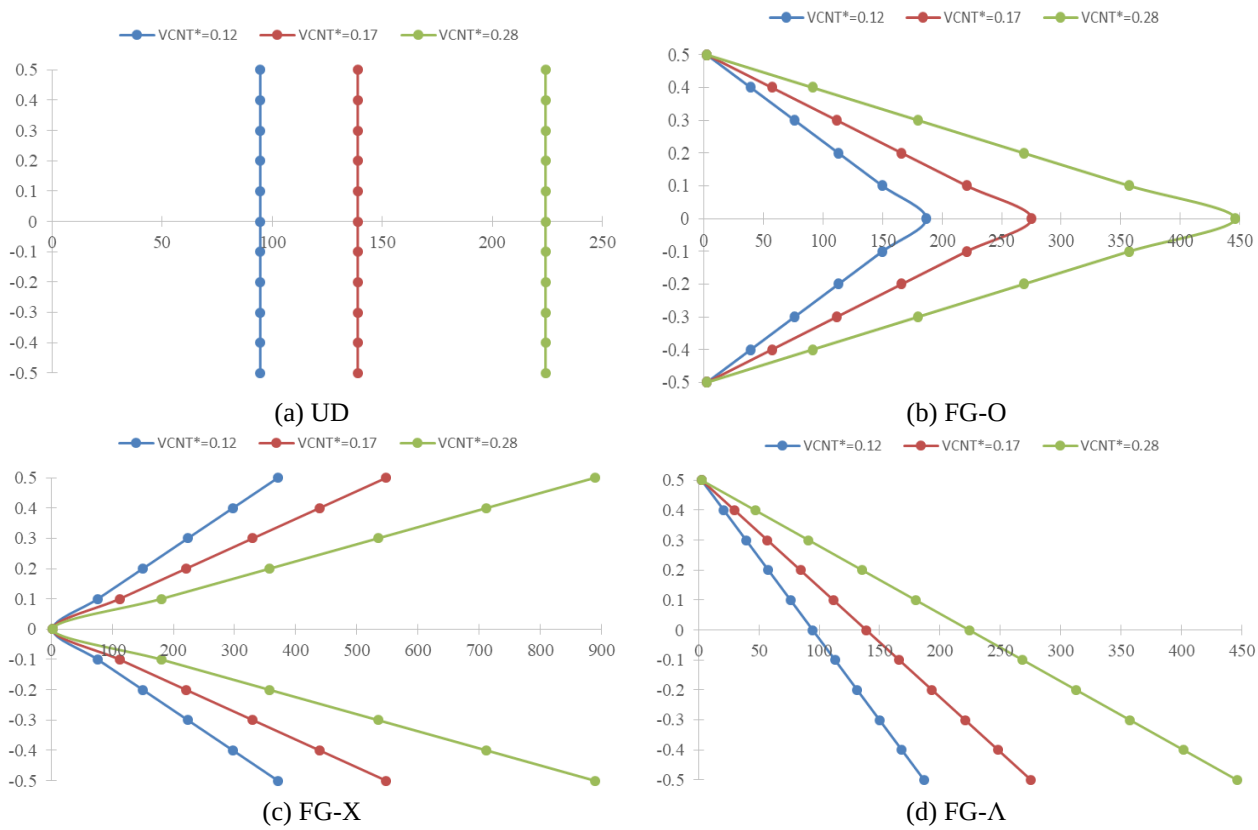

(a) UD (b) FG-O

(c) FG-X (d) FG-Λ

Fig. 2 Longitudinal Young's modulus distribution thought the thickness of FG-CNTRC nanobeams

Table 2 Comparison of non-dimensional first five frequency parameters of FG-CNTRC nanobeams at V_{CNT}* = 0.12

Boundary conditions	CNT distribution	Theory	$\bar{\omega}_1$	$\bar{\omega}_2$	$\bar{\omega}_3$	$\bar{\omega}_4$	$\bar{\omega}_5$
SS	UD	Present	1.0256	3.0475	5.2589	7.5812	9.9802
		Ritz	1.0208	3.0022	5.0854	7.1349	9.1551
		FEM	1.0247	3.0473	5.2566	7.5561	9.9790
	FG-X	Present	1.1820	3.2725	5.4743	7.7541	10.1572
		Ritz	1.1666	3.2182	5.2907	7.3180	9.3193
		FEM	1.1710	3.2664	5.4683	7.7491	10.1560
	FG-O	Present	0.7985	2.6133	4.7896	7.1285	9.6014
		Ritz	0.7883	2.5681	4.6303	6.7224	8.7968
		FEM	0.7914	2.6075	4.7869	7.1209	9.5924
	FG-Λ	Present	0.9953	2.8077	5.0438	7.3376	9.8111
		Ritz	0.9896	2.7625	4.8746	6.9246	8.9902
		FEM	0.9940	2.8040	5.0398	7.3330	9.8017
CC	UD	Present	1.5902	3.3346	5.4109	7.6566	10.1008
		Ritz	1.5759	3.2735	5.2170	7.1953	9.1874
		FEM	1.5874	3.3314	5.4075	7.6482	10.0622
	FG-X	Present	1.6952	3.4688	5.5718	7.8196	10.2303
		Ritz	1.6705	3.4054	5.3751	7.3529	9.3381
		FEM	1.6813	3.4629	5.5688	7.8123	10.2227
	FG-O	Present	1.4040	3.0787	5.0896	7.3131	9.7477
		Ritz	1.3779	3.0042	4.8906	6.8649	8.8776
		FEM	1.3904	3.0635	5.0763	7.3058	9.7346

Table 2 Continued

Boundary conditions	CNT distribution	Theory	$\bar{\omega}_1$	$\bar{\omega}_2$	$\bar{\omega}_3$	$\bar{\omega}_4$	$\bar{\omega}_5$
CC	FG-Λ	Present	1.4912	3.2346	5.2473	7.5201	9.9352
		Ritz	1.4702	3.1324	5.0486	7.0304	9.0385
		FEM	1.4824	3.1911	5.2364	7.4770	9.9046
CF	UD	Present	0.3951	1.7905	3.3142	6.1213	8.5046
		Ritz	0.3942	1.7778	3.8283	5.8895	7.9558
		FEM	0.3947	1.7899	3.9010	6.1165	8.4672
	FG-X	Present	0.4631	1.9477	4.1357	6.3410	8.7035
		Ritz	0.4623	1.9327	4.0487	6.1024	8.1561
		FEM	0.4629	1.9451	4.1262	6.3390	8.6833
	FG-O	Present	0.2949	1.5074	3.4652	5.6513	8.0148
		Ritz	0.2943	1.4923	3.3955	5.4395	7.5290
		FEM	0.2947	1.5036	3.4605	5.6475	8.0086
	FG-Λ	Present	0.3354	1.6316	3.6618	5.8781	8.2305
		Ritz	0.3345	1.6180	3.5920	5.6518	7.7351
		FEM	0.3350	1.6297	3.6602	5.8677	8.2265

Table 3 Comparison of non-dimensional first five frequency parameters of FG-CNTRC nanobeams at V_{CNT}* = 0.17

Boundary conditions	CNT distribution	Theory	$\bar{\omega}_1$	$\bar{\omega}_2$	$\bar{\omega}_3$	$\bar{\omega}_4$	$\bar{\omega}_5$
SS	UD	Present	1.2614	3.8532	6.7277	9.7316	12.9085
		FEM	1.2603	3.8439	6.7213	9.7284	12.8969
	FG-X	Present	1.4312	4.1659	7.0550	10.0485	13.2023
		FEM	1.4515	4.1595	7.0469	10.0414	13.1988
	FG-O	Present	0.9656	3.2468	6.0618	9.1100	12.3505
		FEM	0.9623	3.2437	6.0564	9.1047	12.3456
	FG-Λ	Present	1.2217	3.5125	6.4233	9.4175	12.6663
		FEM	1.2202	3.5075	6.4157	9.4123	12.6570
CC	UD	Present	2.0200	4.2760	6.9632	9.8845	13.0252
		FEM	2.0130	4.2652	6.9521	9.8692	13.0178
	FG-X	Present	2.1612	4.4735	7.2148	10.1486	13.3176
		FEM	2.1514	4.4622	7.2030	10.1376	13.2934
	FG-O	Present	1.7459	3.9012	6.5074	9.4015	12.5783
		FEM	1.7400	3.8920	6.4925	9.3916	12.5629
	FG-Λ	Present	1.8714	4.1025	6.7243	9.6425	12.8299
		FEM	1.8663	4.0718	6.7191	9.6387	12.8125
CF	UD	Present	0.5012	2.2546	4.9825	7.7543	10.9212
		FEM	0.4810	2.2470	4.9553	7.8387	10.9052
	FG-X	Present	0.5802	2.4768	5.2936	8.2212	11.2608
		FEM	0.5673	2.4619	5.2803	8.1793	11.2504
	FG-O	Present	0.3682	1.8808	4.3679	7.1989	10.1783
		FEM	0.3561	1.8632	4.3536	7.1835	10.2605
	FG-Λ	Present	0.4169	2.0319	4.6325	7.5014	10.5896
		FEM	0.4055	2.0303	4.6258	7.4934	10.5710

Table 4 Comparison of non-dimensional first five frequency parameters of FG-CNTRC nanobeams at V_{CNT}*=0.28

Boundary conditions	CNT distribution	Theory	$\bar{\omega}_1$	$\bar{\omega}_2$	$\bar{\omega}_3$	$\bar{\omega}_4$	$\bar{\omega}_5$
SS	UD	Present	1.5203	4.3827	7.4486	10.6277	13.9831
		FEM	1.5097	4.3677	7.4327	10.6136	13.9666
	FG-X	Present	1.7450	4.7314	7.8409	11.0722	14.4659
		FEM	1.7265	4.7168	7.8288	11.0514	14.4550
	FG-O	Present	1.1849	3.8274	6.9795	10.2416	13.7368
		FEM	1.1760	3.8132	6.9626	10.2296	13.7247
	FG-Λ	Present	1.4863	4.0969	7.2730	10.5148	14.0019
		FEM	1.4714	4.0825	7.2588	10.5062	13.9944
CC	UD	Present	2.2792	4.7152	7.6138	10.7322	14.0802
		FEM	2.2631	4.7070	7.6087	10.7218	14.0710
	FG-X	Present	2.4305	4.9701	7.9639	11.1388	14.5514
		FEM	2.4193	4.9599	7.9534	11.1311	14.5436
	FG-O	Present	2.0360	4.4278	7.3011	10.4758	13.9172
		FEM	2.0251	4.4197	7.2938	10.4633	13.9078
	FG-Λ	Present	2.1602	4.5992	7.5162	10.6934	14.1376
		FEM	2.1496	4.5899	7.5064	10.6874	14.1275
CF	UD	Present	0.5969	2.5903	5.5678	8.6399	11.9020
		FEM	0.5878	2.5799	5.5557	8.6321	11.8918
	FG-X	Present	0.6904	2.8298	5.9473	9.0722	12.3927
		FEM	0.6891	2.8233	5.9393	9.0686	12.3858
	FG-O	Present	0.4456	2.2104	5.0276	8.1480	11.5010
		FEM	0.4400	2.2050	5.0247	8.1421	11.4933
	FG-Λ	Present	0.5012	2.3806	5.3001	8.4410	11.7894
		FEM	0.4989	2.3799	5.2970	8.4354	11.7806

compared FEM results by Kumar and Srinivas (2017) for different boundary conditions. As illustrated in Tables 2-4 show good agreement to reference results FEM and Ritz approximate.

It is found that the FG-X nanobeams have the highest natural frequencies, while FG-O nanobeams have the lowest natural frequencies at each boundary conditions. It can be seen the non-dimensional frequency parameters increase with increasing in the volume fraction "V_{CNT}*" of CNTs. Graded CNTs with symmetrical distributions across the beam thickness appear to have higher ability to reduce or increase frequency parameters compared to volume fractions, homogeneous and asymmetrical distributions.

Then, a parametric study is carried out for laminated FG-CNTRC nanobeams. For the material properties are selected the same as the previous examples. The representation of first three non-dimensional natural frequency parameters of two layer cross-ply (0º/90º) FG-CNTRC nanobeams are given in Table 5 for case of V_{CNT}*=0.12 and different boundary conditions. Similar to results in Table 5, for each boundary conditions, the FG-X nanobeams has the largest non-dimensional natural frequencies parameters while the FG-O nanobeams has the smallest non-dimensional natural frequencies parameters.

Table 5 Comparison of non-dimensional first three frequency parameters of cross-ply (0º/90º) FG-CNTRC nanobeams at V_{CNT}* = 0.12

Boundary conditions	CNT distribution	$\bar{\omega}_1$	$\bar{\omega}_2$	$\bar{\omega}_3$
SS	UD	0.6583	1.6907	3.5201
	FG-X	0.7145	1.8922	3.8052
	FG-O	0.5862	1.4202	3.1165
	FG-Λ	0.5310	1.4816	3.1169
CC	UD	0.9401	2.2645	3.9645
	FG-X	1.1052	2.5343	4.2285
	FG-O	0.8142	2.0102	3.5142
	FG-Λ	0.8263	2.1245	3.5963
CF	UD	0.1713	0.9986	2.4214
	FG-X	0.2112	1.2121	2.6612
	FG-O	0.1472	0.9125	2.1743
	FG-Λ	0.1516	0.8406	2.1420

Table 6 provides the non-dimensional natural frequency parameters of three layer cross-ply (0º/90º/0º) FG-CNTRC nanobeams for case of V_{CNT}* = 0.12 and different boundary

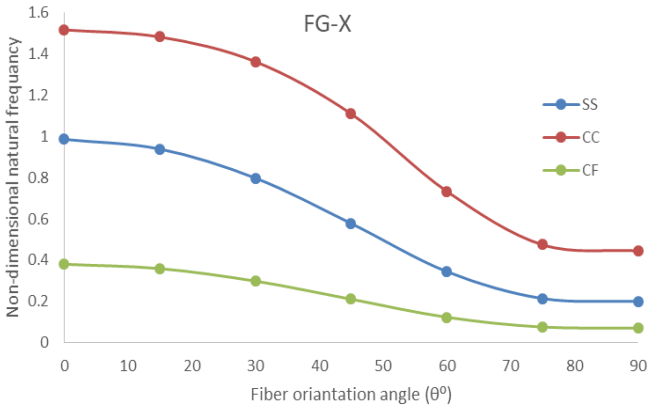

(a) FG-X

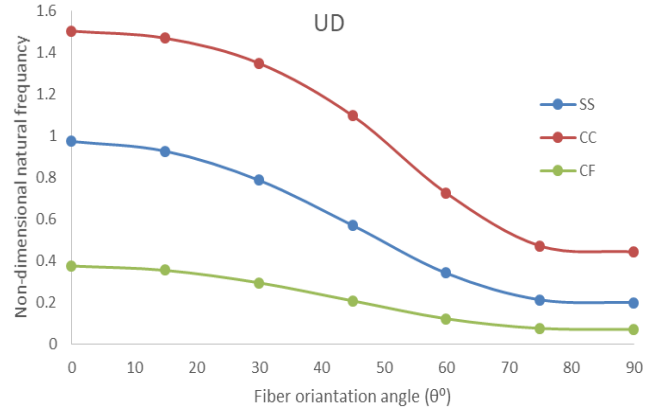

(b) UD

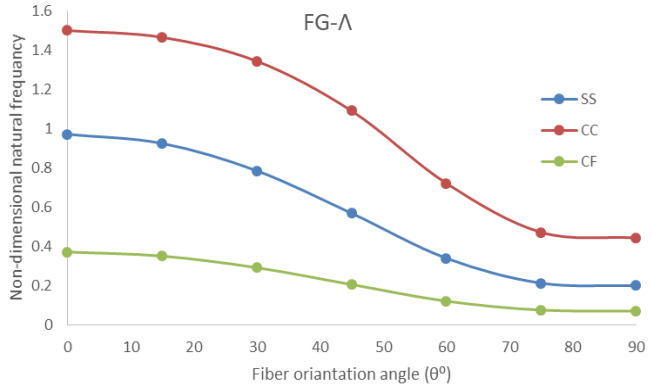

(c) FG-Λ

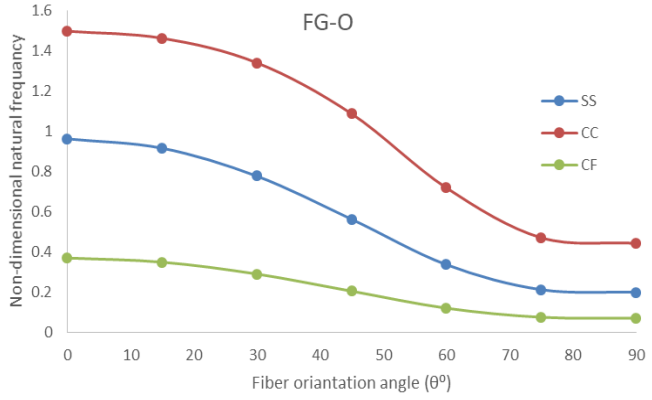

(d) FG-O

Fig. 2 The first non-dimensional natural frequency of four layer (θº/- θº/ -θº/ θº) FG-CNTRC nanobeams

Table 6 Comparison of non-dimensional first three frequency parameters of cross-ply (0º/90º/0º) FG-CNTRC nanobeams at VCNT* = 0.12

Boundary conditions	CNT distribution	$\bar{\omega}_1$	$\bar{\omega}_2$	$\bar{\omega}_3$
SS	UD	0.9723	2.8622	4.8644
	FG-X	0.9852	2.8861	4.8952
	FG-O	0.9574	2.8433	4.8533
	FG-Λ	0.9713	2.8511	4.8619
CC	UD	1.5048	3.2115	4.9936
	FG-X	1.5152	3.2442	5.1089
	FG-O	1.4981	3.2139	4.9897
	FG-Λ	1.5023	3.2166	4.9914
CF	UD	0.3805	1.6933	3.6545
	FG-X	0.3889	1.7014	3.6801
	FG-O	0.3745	1.6817	3.6363
	FG-Λ	0.3765	1.6865	3.6442

conditions. It can be seen that the non-dimensional natural frequency parameters of FG-O→FG-Λ→UD→FG-X nanobeams increasing for all boundary conditions, respectively.

Fig. 2 provides the non-dimensional frequency of four layered (θº/-θº/-θº/θº) FG-CNTRC nanobeams for different boundary conditions and V_{CNT}* = 0.12 with various CNTs orientation angles.

5. Conclusions

Dynamic characteristics of beams made up of FG-CNTRC nanobeams with have been illustrated using the trigonometric shear deformation theory. Nanobeams were considered to have a combination of FG-CNTRC and FG-CNTRC layers with single-walled CNT. The effective material properties were obtained from the rule of mixture by taking into account four types of volume distribution models using micromechanics theory. The equations of motion have been determined through the Hamilton's principle. Gâteaux differential method is employed to obtain the energy functional of FG-CNTRC nanobeams. A mixed FEM formulation is utilized for the formulation of free vibration problems of FG-CNTRC nanobeams with different boundary conditions. Thanks to the GDM, the compatibility of the field equations was checked, and the field equations and boundary conditions were reflected to the functions in a solid way. Thanks to the MFEM, the freedoms were obtained in one go.

The obtained results show that: the form of distribution of reinforcements can affect the stiffness of beams and it is thus expected that the desired stiffness can be achieved by adjusting the distribution of CNTs along the thickness direction of beams. The beams with FG-X distribution have higher fundamental frequency in comparison with other distributions. The investigation on the effect of boundary conditions reveals C-C nanobeams have the greatest natural

frequency parameters. The number of layers increases the frequency of the FG-O and FG-Λ nanobeams increase, while that of the FG-X nanobeams decreases.

Acknowledgments

The research described in this paper was no financially supported.

References

Ahmed Houari, M.S., Benyoucef, S., Mechab, I., Tounsi, A. and Adda Bedia, E.A. (2011), "Two-variable refined plate theory for thermoelastic bending analysis of functionally graded sandwich plates", *J. Therm. Stresses*, **34**(4), 315-334. https://doi.org/10.1080/01495739.2010.550806.

Akbaş, Ş.D. (2016), "Analytical solutions for static bending of edge cracked micro beams", *Struct. Eng. Mech.*, **59**(3), 579-599. http://doi.org/10.12989/sem.2016.59.3.579.

Akbas, S.D. (2018), "Forced vibration analysis of cracked functionally graded microbeams", *Adv. Nano Res.*, **6**(1), 39. http://doi.org/10.12989/anr.2018.6.1.039.

Aköz, A. and Kadioğlu, F. (1996), "The mixed finite element solution of circular beam on elastic foundation", *Comput. Struct.*, **60**(4), 643-651. https://doi.org/10.1016/0045-7949(95)00418-1.

Aköz, Y. and Kadioğlu, F. (1999), "The mixed finite element method for the quasi-static and dynamic analysis of viscoelastic timoshenko beams", *Int. J. Numer. Meth. Eng.*, **44**(12), 1909-1932.https://doi.org/10.1002/(SICI)1097-0207(19990430)44:12<1909::AID-NME573>3.0.CO;2-P.

Al-Furjan, M., Habibi, M., Chen, G., Safarpour, H., Safarpour, M. and Tounsi, A. (2020a), "Chaotic simulation of the multi-phase reinforced thermo-elastic disk using GDQM", *Eng. Comput.*, 1-24. https://doi.org/10.1007/s00366-020-01144-2.

Al-Furjan, M., Habibi, M., Ni, J., won Jung, D. and Tounsi, A. (2020b), "Frequency simulation of viscoelastic multi-phase reinforced fully symmetric systems", *Eng. Comput.*, 1-17. https://doi.org/10.1007/s00366-020-01200-x.

Al-Furjan, M., Safarpour, H., Habibi, M., Safarpour, M. and Tounsi, A. (2020c), "A comprehensive computational approach for nonlinear thermal instability of the electrically FG-GPLRC disk based on GDQ method", *Eng. Comput.*, 1-18. https://doi.org/10.1007/s00366-020-01088-7.

Al-Furjan, M., Habibi, M., Ghabussi, A., Safarpour, H., Safarpour, M. and Tounsi, A. (2021a), "Non-polynomial framework for stress and strain response of the FG-GPLRC disk using three-dimensional refined higher-order theory", *Eng. Struct.*, **228**, 111496. https://doi.org/10.1016/j.engstruct.2020.111496.

Al-Furjan, M., Habibi, M., Shan, L. and Tounsi, A. (2021b), "On the vibrations of the imperfect sandwich higher-order disk with a lactic core using generalize differential quadrature method", *Compos. Struct.*, **257**, 113150. https://doi.org/10.1016/j.compstruct.2020.113150.

Alibeigloo, A. (2014), "Free vibration analysis of functionally graded carbon nanotube-reinforced composite cylindrical panel embedded in piezoelectric layers by using theory of elasticity", *Eur. J. Mech. A Solid*, **44**, 104-115. https://doi.org/10.1016/j.euromechsol.2013.10.002.

Ambartsumian, S. (1958), "On the theory of bending plates", *Izv Otd Tech Nauk AN SSSR*, **5**(5), 69-77.

Arani, A.G., Pourjamshidian, M. and Arefi, M. (2018), "Non-linear free and forced vibration analysis of sandwich nano-beam with FG-CNTRC face-sheets based on nonlocal strain gradient theory", *Smart Struct. Sys.*, **22**(1), 105-120. http://doi.org/10.12989/sss.2018.22.1.105.

Arani, A.G., Pourjamshidian, M., Arefi, M. and Arani, M. (2019), "Thermal, electrical and mechanical buckling loads of sandwich nano-beams made of FG-CNTRC resting on Pasternak's foundation based on higher order shear deformation theory", *Struct. Eng. Mech.*, **69**(4), 439-455. http://doi.org/10.12989/sem.2019.69.4.439.

Arefi, M., Mohammadi, M., Tabatabaeian, A., Dimitri, R. and Tornabene, F. (2018), "Two-dimensional thermo-elastic analysis of FG-CNTRC cylindrical pressure vessels", *Steel Compos. Struct.*, **27**(4), 525-536. http://doi.org/10.12989/scs.2018.27.4.525.

Arefi, M., Pourjamshidian, M. and Arani, A.G. (2019), "Dynamic instability region analysis of sandwich piezoelectric nano-beam with FG-CNTRCs face-sheets based on various high-order shear deformation and nonlocal strain gradient theory", *Steel Compos. Struct.*, **32**(2), 157-171. http://doi.org/10.12989/scs.2019.32.2.151.

Aribas, U.N., Ermis, M., Eratli, N. and Omurtag, M.H. (2019), "The static and dynamic analyses of warping included composite exact conical helix by mixed FEM", *Compos. Part B Eng.*, **160**, 285-297. https://doi.org/10.1016/j.compositesb.2018.10.018.

Arshid, E., Khorasani, M., Soleimani-Javid, Z., Amir, S. and Tounsi, A. (2021), "Porosity-dependent vibration analysis of FG microplates embedded by polymeric nanocomposite patches considering hygrothermal effect via an innovative plate theory", *Eng. Comput.*, 1-22. https://doi.org/10.1007/s00366-021-01382-y.

Asghar, S., Naeem, M.N., Hussain, M., Taj, M. and Tounsi, A. (2020a), "Prediction and assessment of nonlocal natural frequencies of DWCNTs: Vibration analysis", *Comput. Concrete*, **25**(2), 133-144. http://doi.org/10.12989/cac.2020.25.2.133.

Asghar, S., Naeem, M.N., Khadimallah, M.A., Hussain, M., Iqbal, Z. and Tounsi, A. (2020b), "Effect of chiral structure for free vibration of DWCNTs: Modal analysis", *Adv. Concrete Construct.*, **9**(6), 577-588. https://doi.org/10.12989/acc.2020.9.6.577.

Aydogdu, M. (2009), "A new shear deformation theory for laminated composite plates", *Compos. Struct.*, **89**(1), 94-101. https://doi.org/10.1016/j.compstruct.2008.07.008.

Balubaid, M., Tounsi, A., Dakhel, B. and Mahmoud, S. (2019), "Free vibration investigation of FG nanoscale plate using nonlocal two variables integral refined plate theory" *Comput. Concrete*, **24**(6), 579-586. https://doi.org/10.12989/cac.2019.24.6.579.

Bellal, M., Hebali, H., Heireche, H., Bousahla, A.A., Tounsi, A., Bourada, F., Mahmoud, S., Bedia, E. and Tounsi, A. (2020), "Buckling behavior of a single-layered graphene sheet resting on viscoelastic medium via nonlocal four-unknown integral model", *Steel Compos. Struct.*, **34**(5), 643-655. https://doi.org/10.12989/scs.2020.34.5.643.

Bendenia, N., Zidour, M., Bousahla, A.A., Bourada, F., Tounsi, A., Benrahou, K.H., Bedia, E., Mahmoud, S. and Tounsi, A. (2020), "Deflections, stresses and free vibration studies of FG-CNT reinforced sandwich plates resting on Pasternak elastic foundation", *Comput. Concrete*, **26**(3), 213-226. https://doi.org/10.12989/cac.2020.26.3.213.

Berghouti, H., Adda Bedia, E., Benkhedda, A. and Tounsi, A. (2019), "Vibration analysis of nonlocal porous nanobeams made of functionally graded material", *Adv. Nano Res.*, **7**(5), 351-364. http://dx.doi.org/10.12989/anr.2019.7.5.351.

Bouazza, M. and Zenkour, A.M. (2020), "Vibration of carbon nanotube-reinforced plates via refined nth-higher-order theory", *Arch. Appl. Mech.*, **90**, 1755-1769.

https://doi.org/10.1007/s00419-020-01694-3.

Bouderba, B., Houari, M.S.A., Tounsi, A. and Mahmoud, S. (2016), "Thermal stability of functionally graded sandwich plates using a simple shear deformation theory", *Struct. Eng. Mech.*, **58**(3), 397-422. http://doi.org/10.12989/sem.2016.58.3.397.

Boukhari, A., Atmane, H.A., Tounsi, A., Adda Bedia, E. and Mahmoud, S. (2016), "An efficient shear deformation theory for wave propagation of functionally graded material plates", *Struct. Eng. Mech.*, **57**(5), 837-859. http://doi.org/10.12989/sem.2016.57.5.837.

Bourada, F., Bousahla, A.A., Tounsi, A., Bedia, E., Mahmoud, S., Benrahou, K.H. and Tounsi, A. (2020), "Stability and dynamic analyses of SW-CNT reinforced concrete beam resting on elastic-foundation", *Comput. Concrete*, **25**(6), 485-495. https://doi.org/10.12989/cac.2020.25.6.485.

Bousahla, A.A., Bourada, F., Mahmoud, S., Tounsi, A., Algarni, A., Bedia, E. and Tounsi, A. (2020), "Buckling and dynamic behavior of the simply supported CNT-RC beams using an integral-first shear deformation theory", *Comput. Concrete*, **25**(2), 155-166. https://doi.org/10.12989/cac.2020.25.2.155.

Boutaleb, S., Benrahou, K.H., Bakora, A., Algarni, A., Bousahla, A.A., Tounsi, A., Tounsi, A. and Mahmoud, S. (2019), "Dynamic analysis of nanosize FG rectangular plates based on simple nonlocal quasi 3D HSDT", *Adv. Nano Res.*, **7**(3), 191. http://doi.org/10.12989/anr.2019.7.3.191.

Carrera, E. (1998), "Mixed layer-wise models for multilayered plates analysis", *Compos. Struct.*, **43**(1), 57-70. https://doi.org/10.1016/S0263-8223(98)00097-X.

Civalek, O., Uzun, B. and Yayli, M.O. (2020), "Frequency, bending and buckling loads of nanobeams with different cross sections", *Adv. Nano Res.*, **9**(2), 91-104. http://doi.org/10.12989/anr.2020.9.2.091.

Desai, Y., Ramtekkar, G. and Shah, A. (2003), "Dynamic analysis of laminated composite plates using a layer-wise mixed finite element model", *Compos. Struct.*, **59**(2), 237-249. https://doi.org/10.1016/S0263-8223(02)00121-6.

Di Sciuva, M. and Sorrenti, M. (2019), "Bending, free vibration and buckling of functionally graded carbon nanotube-reinforced sandwich plates, using the extended Refined Zigzag Theory", *Compos. Struct.*, **227**, 111324. https://doi.org/10.1016/j.compstruct.2019.111324.

Ebrahimi, F. and Rostami, P. (2018), "Propagation of elastic waves in thermally affected embedded carbon-nanotube-reinforced composite beams via various shear deformation plate theories", *Struct. Eng. Mech.*, **66**(4), 495-504. http://doi.org/10.12989/sem.2018.66.4.495.

Ebrahimi, F., Nouraei, M., Dabbagh, A. and Civalek, O. (2019), "Buckling analysis of graphene oxide powder-reinforced nanocomposite beams subjected to non-uniform magnetic field", *Struct. Eng. Mech.*, **71**(4), 351-361. http://doi.org/10.12989/sem.2019.71.4.351.

Emdadi, M., Mohammadimehr, M. and Navi, B.R. (2019), "Free vibration of an annular sandwich plate with CNTRC facesheets and FG porous cores using Ritz method", *Adv. Nano Res.*, **7**(2), 109. http://doi.org/10.12989/anr.2019.7.2.109.

Farazin, A. and Mohammadimehr, M. (2020), "Nano research for investigating the effect of SWCNTs dimensions on the properties of the simulated nanocomposites: a molecular dynamics simulation", *Adv. Nano Res.*, **9**(2), 83-90. http://doi.org/10.12989/anr.2020.9.2.083.

Feng, H., Shen, D. and Tahouneh, V. (2020), "Vibration analysis of sandwich sector plate with porous core and functionally graded wavy carbon nanotube-reinforced layers", *Steel Compos. Struct.*, **37**(6), 711. https://doi.org/10.12989/scs.2020.37.6.711.

Gemi, L., Yazman, S., Uludağ, M., Dispinar, D. and Tiryakioğlu, M. (2017), "The effect of 0.5 wt% additions of carbon nanotubes & ceramic nanoparticles on tensile properties of epoxy-matrix composites: a comparative study", *Mater. Sci. Nanotechnol.*, **1**(2), 15-22. http://doi.org/10.35841/nanotechnology.1.2.15-22.

Grover, N., Maiti, D. and Singh, B. (2013), "A new inverse hyperbolic shear deformation theory for static and buckling analysis of laminated composite and sandwich plates", *Compos. Struct.*, **95**, 667-675. https://doi.org/10.1016/j.compstruct.2012.08.012.

Grover, N., Maiti, D. and Singh, B. (2014), "An efficient C 0 finite element modeling of an inverse hyperbolic shear deformation theory for the flexural and stability analysis of laminated composite and sandwich plates", *Finite Elem. Anal. Des.*, **80**, 11-22. https://doi.org/10.1016/j.finel.2013.11.003.

Hadji, L., Atmane, H.A., Tounsi, A., Mechab, I. and Bedia, E.A. (2011), "Free vibration of functionally graded sandwich plates using four-variable refined plate theory", *Appl. Math. Mech.*, **32**(7), 925-942. https://doi.org/10.1007/s10483-011-1470-9.

Heidari, F., Afsari, A. and Janghorban, M. (2020), "Several models for bending and buckling behaviors of FG-CNTRCs with piezoelectric layers including size effects", *Adv. Nano Res.*, **9**(3), 193-210. http://doi.org/10.12989/anr.2020.9.3.193.

Heidari, F., Taheri, K., Sheybani, M., Janghorban, M. and Tounsi, A. (2021), "On the mechanics of nanocomposites reinforced by wavy/defected/aggregated nanotubes", *Steel Compos. Struct.*, **38**(5), 533-545. https://doi.org/10.12989/scs.2021.38.5.533.

Hu, H., Onyebueke, L. and Abatan, A. (2010), "Characterizing and modeling mechanical properties of nanocomposites-review and evaluation", *J. Miner. Mater. Charact. Eng.*, **9**(4), 275. https://doi.org/10.4236/jmmce.2010.94022.

Huang, X., Hao, H., Oslub, K., Habibi, M. and Tounsi, A. (2021), "Dynamic stability/instability simulation of the rotary size-dependent functionally graded microsystem", *Eng. Comput.*, 1-17. https://doi.org/10.1007/s00366-021-01399-3.

Hussain, M., Naeem, M.N., Tounsi, A. and Taj, M. (2019), "Nonlocal effect on the vibration of armchair and zigzag SWCNTs with bending rigidity", *Adv. Nano Res.*, **7**(6), 431-442. http://doi.org/10.12989/anr.2019.7.6.431.

Hussain, M., Naeem, M.N. and Tounsi, A. (2020), "Numerical Study for nonlocal vibration of orthotropic SWCNTs based on Kelvin's model", *Adv. Concrete Construct.*, **9**(3), 301-312. https://doi.org/10.12989/acc.2020.9.3.301.

Iijima, S. and Ichihashi, T. (1993), "Single-shell carbon nanotubes of 1-nm diameter", *Nature*, **363**(6430), 603-605. https://doi.org/10.1038/363603a0.

Jamali, M., Shojaee, T., Mohammadi, B. and Kolahchi, R. (2019), "Cut out effect on nonlinear post-buckling behavior of FG-CNTRC micro plate subjected to magnetic field via FSDT", *Adv. Nano Res.*, **7**(6), 405-417. http://dx.doi.org/10.12989/anr.2019.7.6.405.

Karama, M., Afaq, K. and Mistou, S. (2003), "Mechanical behaviour of laminated composite beam by the new multi-layered laminated composite structures model with transverse shear stress continuity", *Int. J. Solid. Struct.*, **40**(6), 1525-1546. https://doi.org/10.1016/S0020-7683(02)00647-9.

Khater, H. and Abd el Gawaad, H. (2016), "Characterization of alkali activated geopolymer mortar doped with MWCNT", *Construct. Building Mater.*, **102**, 329-337. https://doi.org/10.1016/j.conbuildmat.2015.10.121.

Kim, Y., Kim, D., Choi, H., Yu, S. and Park, K. (2017), "Fatigue performance of deepwater steel catenary riser considering nonlinear soil", *Struct. Eng. Mech.*, **61**(6), 737-746. http://doi.org/10.12989/sem.2017.61.6.737.

Kolahdouzan, F., Arani, A.G. and Abdollahian, M. (2018), "Buckling and free vibration analysis of FG-CNTRC-micro sandwich plate", *Steel Compos. Struct.*, **26**(3), 273-287. https://doi.org/10.12989/scs.2018.26.3.273.

Kumar, P. and Srinivas, J. (2017), "Free vibration, bending and buckling of a FG-CNT reinforced composite beam: Comparative analysis with hybrid laminated composite beam", *Multidiscipline Model. Mater. Struct.*, **13**(4), 590-611. https://doi.org/10.1108/MMMS-05-2017-0032.

Lage, R.G., Soares, C.M., Soares, C.M. and Reddy, J. (2004), "Analysis of adaptive plate structures by mixed layerwise finite elements", *Compos. Struct.*, **66**(1), 269-276. https://doi.org/10.1016/j.compstruct.2004.04.048.

Liew, K., Lei, Z. and Zhang, L. (2015), "Mechanical analysis of functionally graded carbon nanotube reinforced composites: a review", *Compos. Struct.*, **120**, 90-97. https://doi.org/10.1016/j.compstruct.2014.09.041.

Lin, F. and Xiang, Y. (2014), "Vibration of carbon nanotube reinforced composite beams based on the first and third order beam theories", *Appl. Math. Model.*, **38**(15), 3741-3754. https://doi.org/10.1016/j.apm.2014.02.008.

Madenci, E. (2019), "A refined functional and mixed formulation to static analyses of fgm beams", *Struct. Eng. Mech.*, **69**(4), 427-437. https://doi.org/10.12989/sem.2019.69.4.427.

Madenci, E. and Gülcü, Ş. (2020), "Optimization of flexure stiffness of FGM beams via artificial neural networks by mixed FEM", *Struct. Eng. Mech.*, **75**(5), 633-642. https://doi.org/10.12989/sem.2020.75.5.633.

Madenci, E. and Özütok, A. (2020), "Variational approximate for high order bending analysis of laminated composite plates", *Struct. Eng. Mech.*, **73**(1), 97-108. https://doi.org/10.12989/sem.2020.73.1.097.

Madenci, E., Özkılıç, Y.O. and Gemi, L. (2020), "Experimental and theoretical investigation on flexure performance of pultruded GFRP composite beams with damage analyses", *Compos. Struct.*, **242**, 112162. https://doi.org/10.1016/j.compstruct.2020.112162.

Mahesh, V. and Harursampath, D. (2020), "Nonlinear deflection analysis of CNT/magneto-electro-elastic smart shells under multi-physics loading", *Mech. Adv. Mater. Struct.*, 1-25. https://doi.org/10.1080/15376494.2020.1805059.

Mahesh, V. and Harursampath, D. (2021), "Large deflection analysis of functionally graded magneto-electro-elastic porous flat panels", *Eng. Comput.*, 1-20. https://doi.org/10.1007/s00366-020-01270-x.

Matouk, H., Bousahla, A.A., Heireche, H., Bourada, F., Bedia, E., Tounsi, A., Mahmoud, S., Tounsi, A. and Benrahou, K. (2020), "Investigation on hygro-thermal vibration of P-FG and symmetric S-FG nanobeam using integral Timoshenko beam theory", *Adv. Nano Res.*, **8**(4), 293-305. https://doi.org/10.12989/anr.2020.8.4.293.

Medani, M., Benahmed, A., Zidour, M., Heireche, H., Tounsi, A., Bousahla, A.A., Tounsi, A. and Mahmoud, S. (2019), "Static and dynamic behavior of (FG-CNT) reinforced porous sandwich plate using energy principle", *Steel Compos. Struct.*, **32**(5), 595-610. https://doi.org/10.12989/scs.2019.32.5.595.

Mehar, K., Panda, S.K. and Mahapatra, T.R. (2017), "Theoretical and experimental investigation of vibration characteristic of carbon nanotube reinforced polymer composite structure", *Int. J. Mech. Sci.*, **133**, 319-329. https://doi.org/10.1016/j.ijmecsci.2017.08.057.

Mehrabadi, S.J., Aragh, B.S., Khoshkhahesh, V. and Taherpour, A. (2012), "Mechanical buckling of nanocomposite rectangular plate reinforced by aligned and straight single-walled carbon nanotubes", *Compos. Part B. Eng.*, **43**(4), 2031-2040. https://doi.org/10.1016/j.compositesb.2012.01.067.

Merdaci, S., Tounsi, A., Houari, M.S.A., Mechab, I., Hebali, H. and Benyoucef, S. (2011), "Two new refined shear displacement models for functionally graded sandwich plates", *Arch. Appl. Mech.*, **81**(11), 1507-1522. https://doi.org/10.1007/s00419-010-0497-5.

Mohammadimehr, M. and Alimirzaei, S. (2017), "Buckling and free vibration analysis of tapered FG-CNTRC micro Reddy beam under longitudinal magnetic field using FEM", *Smart Struct. Syst.*, **19**(3), 309-322. https://doi.org/10.12989/sss.2017.19.3.309.

Moradi-Dastjerdi, R. (2016), "Wave propagation in functionally graded composite cylinders reinforced by aggregated carbon nanotube", *Struct. Eng. Mech.*, **57**(3), 441-456. http://doi.org/10.12989/sem.2016.57.3.441.

Oden, J.T. and Reddy, J.N. (1976), "On mixed finite element approximations", *SIAM J. Numer. Anal.*, **13**(3), 393-404. https://doi.org/10.1137/0713035.

Ouakad, H.M., Sedighi, H.M. and Al-Qahtani, H.M. (2020), "Forward and backward whirling of a spinning nanotube nano-rotor assuming gyroscopic effects", *Adv. Nano Res.*, **8**(3), 245-254. http://doi.org/10.12989/anr.2020.8.3.245.

Özütok, A. and Madenci, E. (2013), "Free vibration analysis of cross-ply laminated composite beams by mixed finite element formulation", *Int. J. Struct. Stabil. Dynam.*, **13**(2), 1250056. https://doi.org/10.1142/S0219455412500563.

Ozutok, A., Madenci, E. and Kadioglu, F. (2014), "Free vibration analysis of angle-ply laminate composite beams by mixed finite element formulation using the Gâteaux differential", *Sci. Eng. Compos. Mater.*, **21**(2), 257-266. https://doi.org/10.1515/secm-2013-0043.

Özütok, A. and Madenci, E. (2017), "Static analysis of laminated composite beams based on higher-order shear deformation theory by using mixed-type finite element method", *Int. J. Mech. Sci.*, **130**, 234-243. https://doi.org/10.1016/j.ijmecsci.2017.06.013.

Phung-Van, P., Abdel-Wahab, M., Liew, K., Bordas, S. and Nguyen-Xuan, H. (2015), "Isogeometric analysis of functionally graded carbon nanotube-reinforced composite plates using higher-order shear deformation theory", *Compos. Struct.*, **123**, 137-149. https://doi.org/10.1016/j.compstruct.2014.12.021.

Rajabi, J. and Mohammadimehr, M. (2019), "Bending analysis of a micro sandwich skew plate using extended Kantorovich method based on Eshelby-Mori-Tanaka approach", *Comput. Concrete*, **23**(5), 361-376. https://doi.org/10.12989/cac.2019.23.5.361.

Reddy, J.N. (1984), "A Simple Higher-Order Theory for Laminated Composite Plates", *J. Appl. Mech.*, **51**(4), 745-752. https://doi.org/10.1115/1.3167719.

Reissner, E. (1975), "On transverse bending of plates, including the effect of transverse shear deformation", *Int. J. Solids Struct.*, **11**(5), 569-573. https://doi.org/10.1016/0020-7683(75)90030-X.

Rouabhia, A., Chikh, A., Bousahla, A.A., Bourada, F., Heireche, H., Tounsi, A., Kouider Halim, B., Tounsi, A. and Al-Zahrani, M.M. (2020), "Physical stability response of a SLGS resting on viscoelastic medium using nonlocal integral first-order theory", *Steel Compos. Struct.*, **37**(6), 695-709. https://doi.org/10.12989/scs.2020.37.6.695.

Shafiei, H. and Setoodeh, A.R. (2017), "Nonlinear free vibration and post-buckling of FG-CNTRC beams on nonlinear foundation", *Steel Compos. Struct.*, **24**(1), 65-77. http://doi.org/10.12989/scs.2017.24.1.065.

Soldatos, K. and Elishakoff, I. (1992), "A transverse shear and normal deformable orthotropic beam theory", *J. Sound Vib.*, **155**(3), 528-533. https://doi.org/10.1016/0022-460X(92)90717-C.

Tahouneh, V. (2017), "Using modified Halpin-Tsai approach for vibrational analysis of thick functionally graded multi-walled carbon nanotube plates", *Steel Compos. Struct.*, **23**(6), 657-668. https://doi.org/10.12989/scs.2017.23.6.657.

Taibi, F.Z., Benyoucef, S., Tounsi, A., Bachir Bouiadjra, R., Adda Bedia, E.A. and Mahmoud, S. (2015), "A simple shear

deformation theory for thermo-mechanical behaviour of functionally graded sandwich plates on elastic foundations", *J. Sandw. Struct. Mater.*, **17**(2), 99-129. https://doi.org/10.1177/1099636214554904.

Torabi, J. and Ansari, R. (2018), "Thermally induced mechanical analysis of temperature-dependent FG-CNTRC conical shells", *Struct. Eng. Mech.*, **68**(3), 313-323. http://doi.org/10.12989/sem.2018.68.3.313.

Tounsi, A., Benguediab, S., Semmah, A. and Zidour, M. (2013), "Nonlocal effects on thermal buckling properties of double-walled carbon nanotubes", *Adv. Nano Res.*, **1**(1), 1-11. http://doi.org/10.12989/anr.2013.1.1.001.

Tounsi, A., Houari, M.S.A. and Bessaim, A. (2016), "A new 3-unknowns non-polynomial plate theory for buckling and vibration of functionally graded sandwich plate", *Struct. Eng. Mech.*, **60**(4), 547-565. https://doi.org/10.12989/sem.2016.60.4.547.

Touratier, M. (1991), "An efficient standard plate theory", *Int. J. Eng. Sci.*, **29**(8), 901-916. https://doi.org/10.1016/0020-7225(91)90165-Y.

Vinyas, M. (2019a), "A higher-order free vibration analysis of carbon nanotube-reinforced magneto-electro-elastic plates using finite element methods", *Compos. Part B Eng.*, **158**, 286-301. https://doi.org/10.1016/j.compositesb.2018.09.086.

Vinyas, M. (2019b), "Vibration control of skew magneto-electro-elastic plates using active constrained layer damping", *Compos. Struct.*, **208**, 600-617. https://doi.org/10.1016/j.compstruct.2018.10.046.

Vinyas, M. (2020a), "Nonlinear deflection of carbon nanotube reinforced multiphase magneto-electro-elastic plates in thermal environment considering pyrocoupling effects", *Math. Method Appl. Sci.* https://doi.org/10.1002/mma.6858.

Vinyas, M. (2020b), "On frequency response of porous functionally graded magneto-electro-elastic circular and annular plates with different electro-magnetic conditions using HSDT", *Compos. Struct.*, **240**, 112044. https://doi.org/10.1016/j.compstruct.2020.112044.

Vinyas, M. (2021), "Porosity effect on the nonlinear deflection of functionally graded magneto-electro-elastic smart shells under combined loading", *Mech. Adv. Mater. Struct.*, 1-27. https://doi.org/10.1080/15376494.2021.1875086.

Vinyas, M. and Dineshkumar, H. (2020), "Nonlinear vibration of functionally graded magneto-electro-elastic higher order plates reinforced by CNTs using FEM", *Eng. Comput.*, 1-23. https://doi.org/10.1007/s00366-020-01098-5.

Vinyas, M. and Harursampath, D. (2020), "Nonlinear vibrations of magneto-electro-elastic doubly curved shells reinforced with carbon nanotubes", *Compos. Struct.*, **253**, 112749. https://doi.org/10.1016/j.compstruct.2020.112749.

Vinyas, M., Nischith, G., Loja, M., Ebrahimi, F. and Duc, N. (2019a), "Numerical analysis of the vibration response of skew magneto-electro-elastic plates based on the higher-order shear deformation theory", *Compos. Struct.*, **214**, 132-142. https://doi.org/10.1016/j.compstruct.2019.02.010.

Vinyas, M., Sunny, K., Harursampath, D., Nguyen-Thoi, T. and Loja, M. (2019b), "Influence of interphase on the multi-physics coupled frequency of three-phase smart magneto-electro-elastic composite plates", *Compos. Struct.*, **226**, 111254. https://doi.org/10.1016/j.compstruct.2019.111254.

Vinyas, M., Harursampath, D. and Thoi, T.N. (2021), "A higher order coupled frequency characteristics study of smart magneto-electro-elastic composite plates with cut-outs using finite element methods", *Defence Technology*, **17**(1), 100-118. https://doi.org/10.1016/j.dt.2020.02.009.

Vodenitcharova, T. and Zhang, L.C. (2006), "Bending and local buckling of a nanocomposite beam reinforced by a single-walled carbon nanotube", *Int. J. Solids Struct.*, **43**(10), 3006-3024. https://doi.org/10.1016/j.ijsolstr.2005.05.014.

Wu, C.P., Chen, Y.H., Hong, Z.L. and Lin, C.H. (2018a), "Nonlinear vibration analysis of an embedded multi-walled carbon nanotube", *Adv. Nano Res.*, **6**(2), 163-182. http://dx.doi.org/10.12989/anr.2018.6.2.163.

Wu, H., Kitipornchai, S. and Yang, J. (2018b), "Free vibration of thermo-electro-mechanically postbuckled FG-CNTRC beams with geometric imperfections", *Steel Compos. Struct.*, **29**(3), 319-332. https://doi.org/10.12989/scs.2018.29.3.319.

Wuite, J. and Adali, S. (2005), "Deflection and stress behaviour of nanocomposite reinforced beams using a multiscale analysis", , *Compos. Struct.*, **71**(3-4), 388-396. https://doi.org/10.1016/j.compstruct.2005.09.011.

Zerrouki, R., Karas, A., Zidour, M., Bousahla, A.A., Tounsi, A., Bourada, F., Tounsi, A., Benrahou, K.H. and Mahmoud, S. (2021), "Effect of nonlinear FG-CNT distribution on mechanical properties of functionally graded nano-composite beam", *Struct. Eng. Mech.*, **78**(2), 117-124. https://doi.org/10.12989/sem.2021.78.2.117.

Zhou, C., Zhang, Z., Zhang, J., Fang, Y. and Tahouneh, V. (2020), "Vibration analysis of FG porous rectangular plates reinforced by graphene platelets", *Steel Compos. Struct.*, **34**(2), 215-226. https://doi.org/10.12989/scs.2020.34.2.215.

Zhu, P., Lei, Z. and Liew, K.M. (2012), "Static and free vibration analyses of carbon nanotube-reinforced composite plates using finite element method with first order shear deformation plate theory", *Compos. Struct.*, **94**(4), 1450-1460. https://doi.org/10.1016/j.compstruct.2011.11.010.

AT